HHS Public Access

Author manuscript

Nature. Author manuscript; available in PMC 2016 December 02.

Published in final edited form as:

Nature. ; 534(7605): 119–123. doi:10.1038/nature17959.

Pitx2 promotes heart repair by activating the antioxidant response after cardiac injury

Ge Tao[1], **Peter C. Kahr**[1], **Yuka Morikawa**[2], **Min Zhang**[1], **Mahdis Rahmani**[2], **Todd R. Heallen**[2], **Lele Li**[1], **Zhao Sun**[3], **Eric N. Olson**[4], **Brad A. Amendt**[3], and **James F. Martin**[1,2,5,6,*]

[1]Department of Molecular Physiology and Biophysics, Baylor College of Medicine, Houston, TX 77030, USA

[2]Texas Heart Institute, Houston, TX 77030, USA

[3]Department of Anatomy and Cell Biology and the Craniofacial Anomalies Research Center, The University of Iowa, Iowa City, IA 52242, USA

[4]Department of Molecular Biology and Hamon Center for Regenerative Science and Medicine, University of Texas Southwestern Medical Center, Dallas, TX 75390-9148

[5]Program in Developmental Biology, Baylor College of Medicine, Houston, TX 77030

[6]Cardiovascular Research Institute, Baylor College of Medicine, Houston, TX 77030

Summary

Myocardial infarction results in compromised myocardial function with heart failure due to insufficient cardiomyocyte self-renewal[1]. Unlike lower vertebrates, mammalian hearts only have a transient neonatal renewal capacity[2]. Reactivating primitive reparative ability in the mature heart requires knowledge of the mechanisms promoting early heart repair. By testing an established Hippo-deficient heart regeneration model for renewal promoting factors, we found that *Pitx2* expression was induced in injured, Hippo-deficient ventricles. *Pitx2*-deficient neonatal hearts failed to repair after apex resection while *Pitx2*-gain-of-function in adult cardiomyocytes conferred reparative ability after myocardial infarction. Genomic analyses indicated that Pitx2 activated genes encoding electron transport chain components and reactive oxygen species scavengers. A subset of Pitx2 target genes was cooperatively regulated with the Hippo effector, Yap. Furthermore, Nrf2, a regulator of antioxidant response[3], directly regulated *Pitx2* expression and

*To whom correspondence should be addressed. jfmartin@bcm.edu.

Author contributions

J.F.M. and G.T. conceived the project and designed the experiments. G.T., P.C.K., Y.M., M.R, T.R.H., L.L. performed experiments and analyzed data. Z.S. and B.A.A. provided reagents and performed experiments. E.N.O. provided transgenic animal model. M.Z. and G.T. performed bioinformatics and statistical analyses. J.F.M supervised the project and analyzed data. G.T. and J.F.M. wrote the manuscript.

Sequencing dataset generated in this manuscript can be assessed at: http://www.ncbi.nlm.nih.gov/geo/query/acc.cgi?token=wfolwmwevdkltcd&acc=GSE70413 Series# GSE70413

Supplementary Materials
Methods
Extended Data Figures and legends 1–10
References (25–33)

subcellular localization. *Pitx2* mutant myocardium had elevated reactive oxygen species levels while antioxidant supplementation suppressed the *Pitx2*-loss-of-function phenotype. These findings reveal a genetic pathway, activated by tissue damage that is essential for cardiac repair.

We used immunofluorescence staining to look for developmental transcription factors that were up-regulated in regenerating Hippo-deficient heart[4]. *Paired-like homeodomain 2* (*Pitx2*) was enriched in border zone ventricular cardiomyocyte nuclei of adult Hippo-deficient hearts after myocardial infarction (MI) (Fig. 1a–c). *Pitx2*, encoding three isoforms (*Pitx2a*, *Pitx2b*, and *Pitx2c*), is mutated in Rieger Syndrome that is characterized by craniofacial, umbilical, and cardiac abnormalities[5] and functions in left-right asymmetric organ development[6]. Notably, *Pitx2* deficiency results in predisposition to atrial fibrillation (AF), a common human arrhythmia[7,8]. *Pitx2c* is the major isoform expressed in heart.

Available RNA-sequencing (RNA-Seq) data indicated that *Pitx2* transcripts in cardiomyocytes dropped postnatally[9] (Fig. 1d) while Western blot revealed Pitx2 protein induction after injury during regenerative stages (Fig. 1e). Consistent with reduced Pitx2 expression in adult hearts, active histone marks at the *Pitx2* locus were reduced in adult hearts (Fig. 1f, g)[10]. Available Dnase I Hypersensitive sequencing (DHS) data revealed that Nrf2 binding-elements were enriched in the *Pitx2* locus (data not shown). To evaluate whether Nrf2 activated *Pitx2* after injury, we performed an Nrf2 Chromatin Immunoprecipitation Sequenceing (ChIP-Seq) experiment on hearts 4 days after postnatal day (P) 2 left anterior descending artery occlusion (LAD-O) and discovered Nrf2 binding at the *Pitx2* locus (Fig. 1f). *Nrf*2 knockdown in P19 cells and *Nrf2* loss-of-function in mice resulted in decreased *Pitx2* mRNA expression supporting the conclusion that Nrf2 directly regulates *Pitx2* after tissue injury (Fig. 1h, i).

We determined whether *Pitx2*, similarly to *Yap*, was required for neonatal heart regeneration[2]. Using muscle creatine kinase cre (MCK^{cre})[11], we inactivated *Pitx2* in cardiomyocytes and performed P1 apex resection. While control hearts regenerated as expected, $MCK^{cre;}$ $Pitx2^{f/f}$ (*Pitx2CKO*) hearts had increased scarring and reduced function (Fig. 2a–e). We injured *Pitx2* mutant hearts by LAD-O at P1 and used both MCK^{cre} and $Myh6^{creERT}$ to inactivate *Pitx2* in myocardium. *Pitx2* mutants failed to repair after LAD-O (Extended Data Fig. 1).

We examined cardiomyocyte proliferation in P1 apex resection model at 5 day-post-resection (DPR) by pulse-labeling and immunofluorescence of 5-ethynyl-2′-deoxyuridine (EdU). In $Pitx2^{f/f}$ controls, injury induced a threefold increase of EdU positive cardiomyocytes compared to sham that was absent in *Pitx2CKO* after injury, supporting the hypothesis that *Pitx2*, like *Yap*, is essential for neonatal heart regeneration by promoting proliferation and injury resistance (Fig. 2f–h).

To investigate whether *Pitx2* is sufficient for adult cardiomyocyte repair, we generated $Pitx2^{Gof}$, a cre-activated *Pitx2c* gain-of-function transgenic line (Extended Data Fig. 2a). Immunoblotting and qPCR showed elevated *Pitx2c* levels in $Myh6^{cre\text{-}Ert}$;$Pitx2^{Gof}$ (*Pitx2OE*) ventricles (Extended Data Fig. 2b–d). LAD-O performed in 8-week-old mice after tamoxifen administration revealed that *Pitx2OE* hearts had reduced scar size (Fig. 2i, j)[4].

Heart morphology was comparable between controls (*Myh6*$^{cre\text{-}Ert/+}$) and *Pitx2OE* after sham surgery (Extended Data Fig. 2e–g). Two weeks after LAD-O both *Pitx2OE* and controls showed decreased ejection fraction (EF) and fractional shortening (FS), however, *Pitx2OE* mice had functional recovery at 3 and 4 weeks-post-LAD-O (Fig. 2k, l). Non-regenerative stage P8 apex resections in control and *Pitx2OE* hearts revealed that *Pitx2*OE hearts had reduced scarring (Extended Data Fig. 2h–j) and improved function at 28 DPR (Extended Data Fig. 2k, l). EdU incorporation at 8 DPR showed increased cardiomyocyte S-phase entry in *Pitx2OE* hearts (Extended Data Fig. 2m–o).

Since *Pitx2* was up-regulated in Hippo-deficient hearts, we tested whether *Pitx2* was required for Hippo-deficient cardiomyocyte renewal. *SalvCKO* hearts regenerate efficiently after MI[4]. However, *SalvCKO* hearts that were also *Pitx2* mutant, called double knock out (*DKO*), failed to regenerate (Fig. 3a–c). Twenty-eight days after P8 LAD-O, *DKO* hearts had a larger scar and compromised EF (Fig. 3d, e)[4]. Apex resection in non-regenerative P8 hearts also revealed the requirement for *Pitx2* function in *SalvCKO* cardiomyocyte renewal (Extended Data Fig. 3).

Available genomic footprinting data from cardiac DHS datasets can uncover sequence-specific transcription factor (TF)-DNA interactions in an unbiased fashion. Motifs for Pitx2 and Tead, the Yap DNA binding partner, were highly enriched in fetal heart footprints and often found in close proximity (Extended Data Fig. 4a, b). Genomic regions containing Pitx2 or Tead motifs were enriched for H3K4me1 chromatin marks indicating that Pitx2 or Tead binding regions were transcriptionally active. Regions containing both Pitx2 and Tead motifs showed globally increased transcriptional activity compared to Pitx2 motif only regions (Extended Data Fig. 4c, d).

The co-occurrence of TF binding motifs often indicates TF interactions. We tested whether Pitx2 was a Yap binding partner using purified Glutathione S-Transferase (GST) fusion proteins. *In vitro* binding assays with Pitx2 fusion peptides and full length Yap revealed that Yap bound the Pitx2 homeodomain (Fig. 3f, g; Extended Data Fig. 5a, b). We uncovered an *in vivo* interaction between endogenous Pitx2 and Yap using co-immunoprecipitation (co-IP) of endogenous cardiac proteins (Extended Data Fig. 5c). The *Pitx2*^{flag} allele, previously generated by gene targeting in embryonic stem cells (ESC), expresses endogenous levels of FLAG-epitope-tagged Pitx2 from the *Pitx2* locus[7].

Immunofluorescence showed widespread distribution of Pitx2 in P19 cells and a cytoplasm-to-nucleus translocation upon H_2O_2 treatment (Fig. 3h, Extended Data Fig. 6a), similar to the Nrf2 response to oxidative stress (Extended Data Fig. 6b)[3]. Pitx2 nuclear translocation after H_2O_2 treatment depended on Nrf2 activity (Fig. 3h, i). In contrast, Nrf2 nuclear translocation after H_2O_2 treatment was intact in Pitx2^{null} P19 cells indicating that Pitx2 was dispensable for Nrf2 response to reactive oxygen species (ROS) (Extended Data Fig. 6b, c). We found that Pitx2 interacts with Nrf2 in heart extracts, expressing endogenous protein levels (Fig. 3j). Co-IP using Nuclear-cytoplasmic fractionation of P19 cells, looking at endogenous proteins, indicated that Pitx2 binding to Nrf2 in the nucleus was increased after H_2O_2 treatment (Extended Data Fig. 6d, e). We also found less nuclear Pitx2 in *Nrf2* mutant hearts after P1 apex resection (Extended Data Fig. 6f–h).

To solidify the connection between Nrf2, Pitx2, and Yap, we tested if Nrf2 was required for neonatal regeneration, as is the case for Pitx2 and Yap. MI at P2 revealed that Nrf2 null hearts were unable to regenerate indicating that induction of the antioxidant response is required for regeneration (Extended Data Fig. 7)[12]. Notably, *Pitx2OE* mice that were heterozygous for $Nrf2^{nu}$ allele failed to regenerate, suggesting that *Pitx2* promotes the antioxidant response. It is also possible that Nrf2 is downstream of Pitx2 in certain contexts. We also made *Pitx2OE* mice that were heterozygous for a Yap^{fl} allele[13]. Reducing *Yap* dosage compromised *Pitx2OE* heart regeneration in P8 resection model (Extended Data Fig. 8a–e).

To investigate *Pitx2* target genes induced by injury, we harvested P1 resected ventricles from $Pitx2^{f/f}$ and *Pitx2CKO* hearts at 5 DPR and performed RNA-Seq (Extended Data Fig. 9a–d). We identified 1002 down-regulated genes in *Pitx2* mutants (fdr ≤ 0.1, fold change ≥ 1.5). There was extensive overlap between up-regulated genes following apex resection in controls and down-regulated genes in 5DPR *Pitx2CKO* hearts, indicating that in the absence of *Pitx2*, a set of stress response genes, including oxidative stress response genes, fail to be activated (Extended Data Fig. 9a–d).

We examined the response of *Pitx2* and antioxidant scavenger genes to H_2O_2 in *Pitx2*-null ($Pitx2^{nu}$) ESCs since *Pitx2* has been implicated in ROS response in skeletal muscle[6,14]. After H_2O_2 treatment, qPCR showed increased *Pitx2*, *Gpx1*, *Mt1* and *Mt2* expression in wild type ESCs, but not $Pitx2^{nu}$ ESCs (Extended Data Fig. 9f) supporting a critical role for *Pitx2* in response to ROS. While ESCs had low endogenous *Pitx2* levels, the mouse P19 embryonic carcinoma cell line expressed readily detectable *Pitx2*, primarily the *Pitx2c* isoform. H_2O_2 treated P19 cells increased *Pitx2* and its target gene expression levels in a dose-dependent manner (Extended Data Fig. 9g, h).

To identify Pitx2 target genes, we performed P1 apex resection and harvested 5 DPR $Pitx2^{flag}$ ventricles and performed ChIP-Seq (Extended Data Fig. 9e). Overlay of down-regulated genes from *Pitx2CKO* RNA-Seq with Pitx2-binding peaks from ChIP-Seq revealed 505 direct Pitx2 targets. Gene Ontology (GO) analysis revealed enrichment in mitochondria, oxidation-reduction, ribosome, and respiratory chain (Fig. 4a, b).

Among *Pitx2* targets were genes that protect the cell from elevated ROS, such as superoxide dismutase genes, *Sod1* and *Sod2*, which reduce superoxide to H_2O_2 and the glutathione peroxidase, *Gpx4*, that removes H_2O_2, and *peroxiredoxin-2* (Fig. 4b)[15]. Pitx2 regulates electron transport chain (ETC) complex-I components including *Ndufb3, Ndufb4*, and *Ndufb7* and ETC complex-IV component, *Cox7c* (Fig.4b). Defective complex-I in human patients increases ROS sensitivity[16]. Pitx2 regulated 21.5% of its direct target genes through promoter binding revealed by enrichment of H3K4me3 chromatin marks for active promoters in Pitx2 peaks (Fig. 4c; 119/505 direct targets). 8-week-old heart H3K4me3 chromatin marks are enriched in the center of Pitx2 binding sites, supporting the hypothesis that Pitx2 promotes transcriptional activation[17].

To determine whether Pitx2 and Yap regulate common target genes, we performed Yap ChIP-Seq on ventricles 5 days after P2 LAD-O and found Yap binding sites enriched in

nearly half of Pitx2-targeted gene promoters (54/119; Fig. 4a, c). Comparison of Pitx2 ChIP-Seq, our Yap ChIP-Seq, and available Yap ChIP-Seq[18–21], revealed 4 redox genes bound by both Pitx2 and Yap. ChIP-re-ChIP assay from heart extracts revealed Pitx2 and Yap were concurrently resident on these genes, indicating Yap and Pitx2 cooperatively activate the transcriptional response to oxidative stress. (Fig. 4d).

To investigate ROS activity in *Pitx2*$^{f/f}$ and *Pitx2CKO* apical border zones at 4 DPR, tissue sections were incubated with ROS-detecting reagent. *Pitx2CKO* hearts had elevated ROS in both cardiomyocytes and non-myocytes (Fig. 4e–i). To determine if elevated ROS contributed to scarring in 21 DPR *Pitx2CKO* hearts, we administrated N-Acetyl-L-cysteine (NAC) in *Pitx2CKO* neonates after apex resection. Daily NAC injections until 10 DPR decreased scar size in *Pitx2CKO* hearts (Fig. 4j–n).

Elevated ROS is a natural response to cardiac injury including ischemic damage (Extended Data Fig. 10)[22,23]. During the postnatal transition from glycolytic to oxidative metabolism, ROS is elevated in the heart and inhibits cardiomyocyte regeneration[22]. In regenerative-stage hearts, Pitx2 promotes regeneration by inhibiting ROS. Injury induces *Pitx2* expression and activity through Nrf2-activated *Pitx2* transcription and nuclear shuttling. In turn, Pitx2 activates ROS scavengers, protecting cells from oxidative damage, and ETC components. It is also possible that Nrf2 also acts downstream of Pitx2 in some contexts. Thus, Pitx2 is essential for cardiomyocyte response to injury and may prevent cell death.

We uncovered a Pitx2-Yap interaction important for Hippo-deficient cardiac regeneration. Pitx2 binds Yap and cooperatively activates genes maintaining redox balance. *Pitx2* gain-of-function, sufficient to confer reparative capacity in adult cardiomyocytes, is repressed by *Yap* heterozygosity. This suggests that Pitx2 recruits Yap to target genes even in contexts when Hippo is active and the pool of nuclear Yap is relatively low. This mechanism may work in parallel to other mechanisms by which Yap protects the cell from ROS[24].

Extended Data

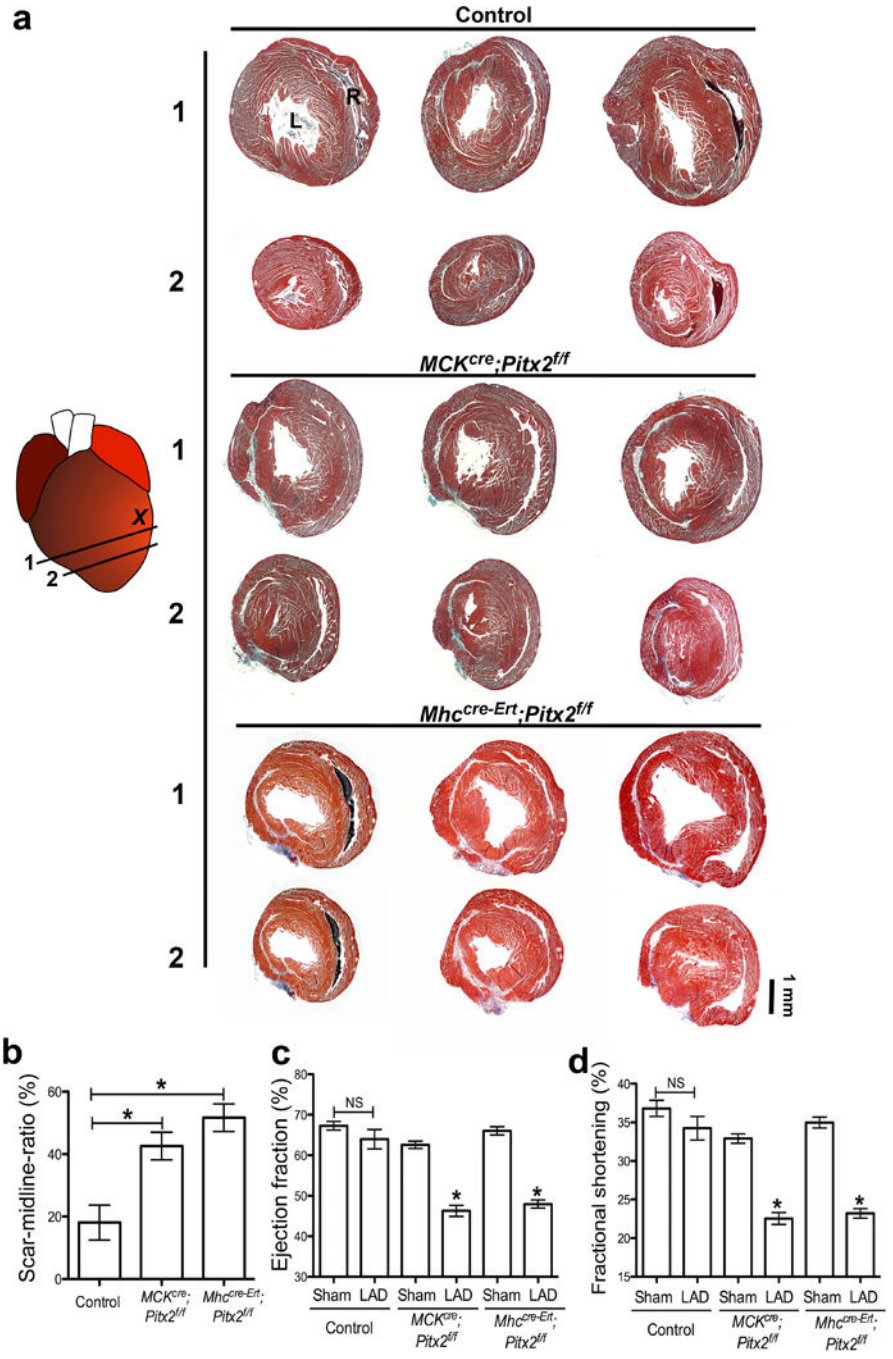

Extended Data Figure 1.

Pitx2 is required in neonatal myocardial regeneration after LAD-O. (a) Serial trichrome images of control (*Pitx2*$^{f/f}$), *MCK*^{cre};*Pitx2*$^{f/f}$, and *Mhc*$^{cre\text{-}Ert}$;*Pitx2*$^{f/f}$ 21 days after LAD-O at P2. (b) Percentage of fibrotic left ventricular myocardium quantified at 3 weeks post-LAD-O, n=4. (c, d) Ejection fraction (c) and fractional shortening (d) of LAD-O and sham hearts.

L, left ventricle; R, right ventricle. Mean ± S.E.M.; Statistical test, (c–d) one-way ANOVA plus Bonferroni post-test; (b) Mann-Whitney. *, p<0.05; NS, not significant.

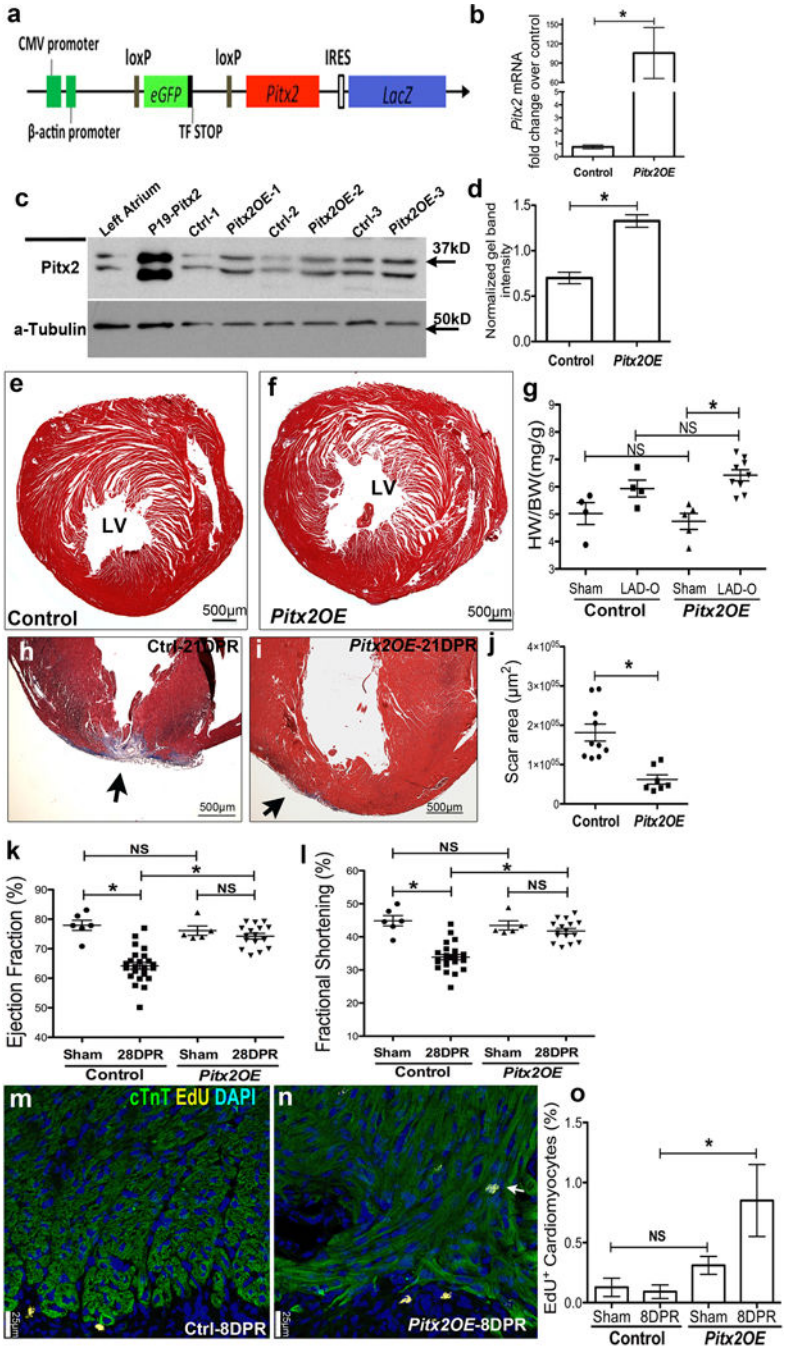

Extended Data Figure 2.

Pitx2 promotes myocardial regeneration after apex resection at P8. (a) Schematic of *Pitx2*-expressing construct (*Pitx2*^{Gof}). (b–d) *Pitx2*^{Gof} was crossed with *Mhc*$^{cre\text{-}Ert}$ strain to generate *Mhc*$^{cre\text{-}Ert/+}$;*pitx2*^{Gof} (*Pitx2OE*), after Tamoxifen treatment, qPCR (b, n=4), western (c, d, n=3) showed the over-expression of *Pitx2* in *Pitx2OE* ventricles. (e–f)

Trichrome-stained cross sections from 13 weeks old sham hearts of control (e) and *Pitx2OE* (f), with tamoxifen administrated at 7–8 weeks old. (g) Heart weight over body weight ratio of adult sham and LAD-O hearts. (h–j) Apex resection of *Pitx2OE* (i) and control (*Mhc*$^{cre\text{-}Ert/+}$) (h) hearts at P8 followed by trichrome staining at 28 DPR, scar area was quantified in j. (k, l) Echocardiography showed ejection fraction (k) and fractional shortening (l) at 28 DPR. (m–o) EdU labeling of *Pitx2OE* (n) and control (m) apical area, 8 days after P8 resection, sections were stained for cTnT (green), EdU (yellow), and DAPI (blue). Arrow indicates EdU-labeled cardiomyocytes, with quantification in o, n=4. Mean ± S.E.M.; Statistical test, (g, k, l) one-way ANOVA plus Bonferroni post-test; (b, d, j, o) Mann-Whitney. *, $p<0.05$; NS, not significant.

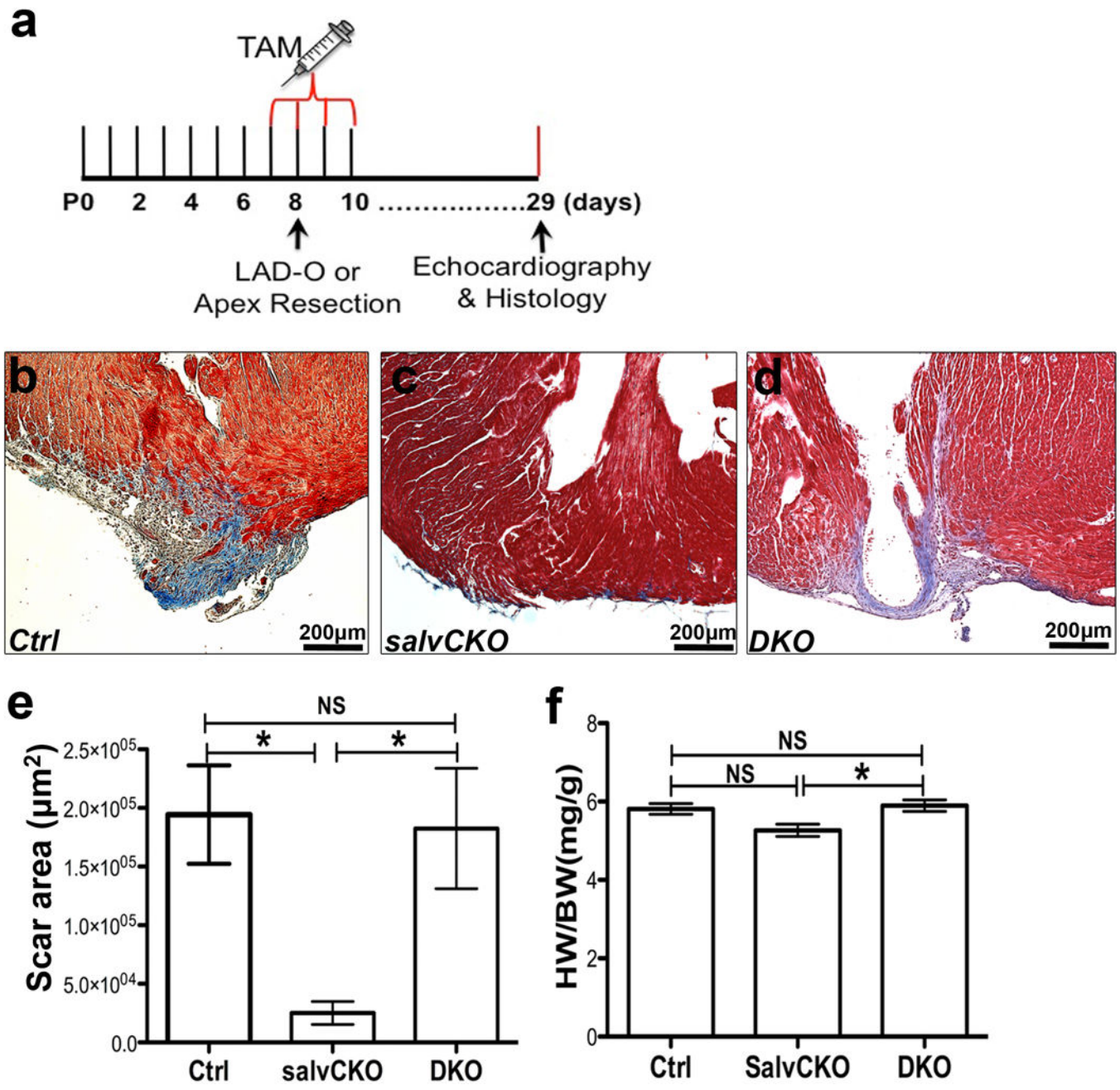

Extended Data Figure 3.

Pitx2 is required for Hippo deficient heart regeneration. (a) Schematic study plan for figure 3a–e. (b–e) Trichrome-stained apical areas of control (b), *SalvCKO* (c) and *DKO* (d) hearts 21 days after P8 apex resection. Scar area was quantified in e. (f) Heart weight to body weight ratio of sham hearts at 28 days after tamoxifen administration. N number, see Methods. Mean ± S.E.M.; Statistical test, (e, f) Mann-Whitney. *, $p<0.05$; NS, not significant.

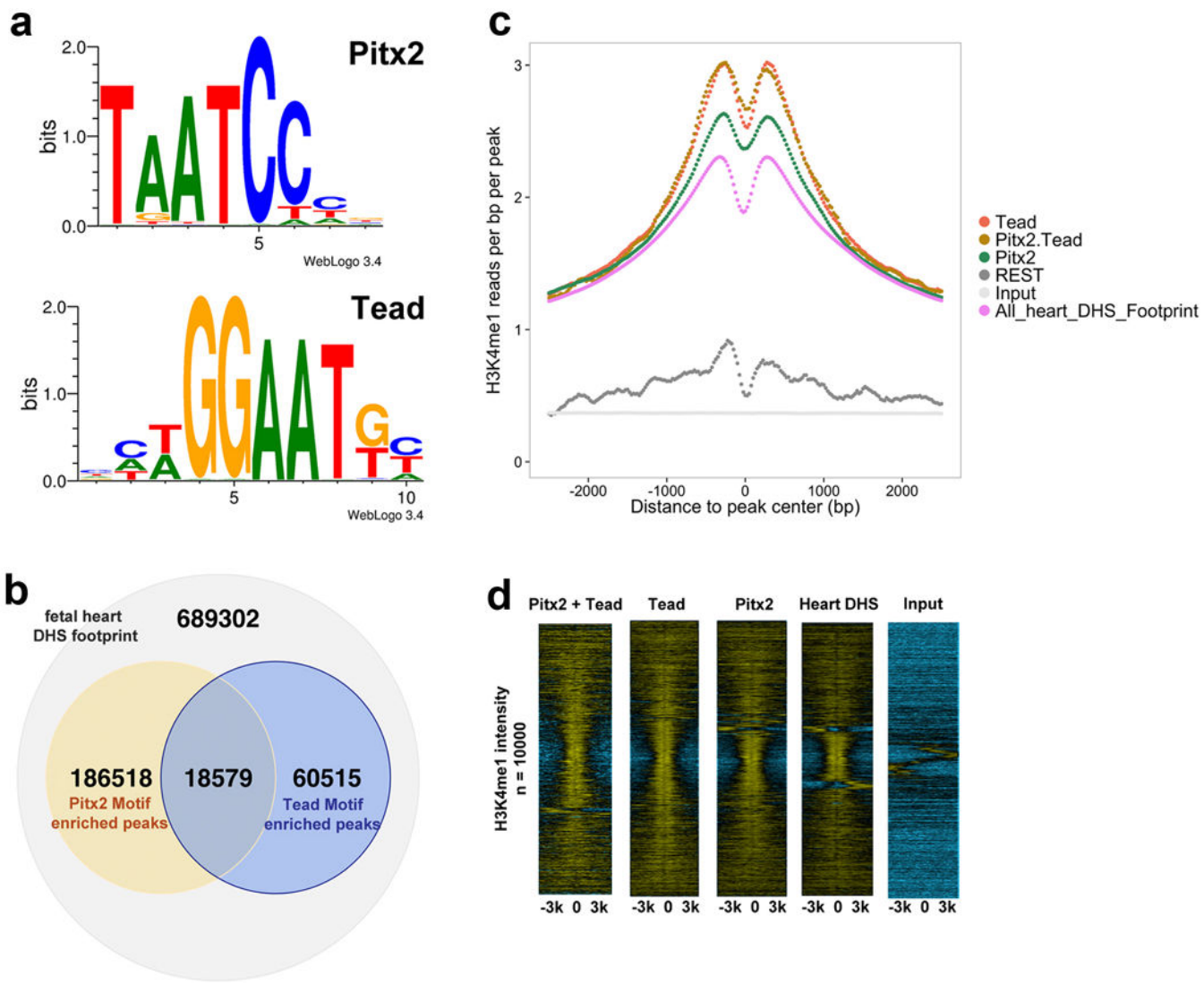

Extended Data Figure 4.

Co-occurrence of Pitx2 and Tead DNA-binding motifs in fetal heart enhancers. (a) Consensus Pitx2 and Tead motifs. (b) Pitx2 and Tead motif co-occurrence in fetal heart Dnase I Hypersensitive (DHS) peaks. (c) Aggregate plot of H3K4me1 in fetal heart ChIP-Seq reads within 6 kb range of DHS peaks. (d) Heat-map of fetal heart H3K4me1 ChIP-Seq or input read density in 6 kb regions of DHS peaks. DHS peaks were centered on Pitx2 motif, Tead motif, Pitx2-Tead motifs, or randomly selected. The read density was in log2 scale; negative values, blue color; positive values, yellow color.

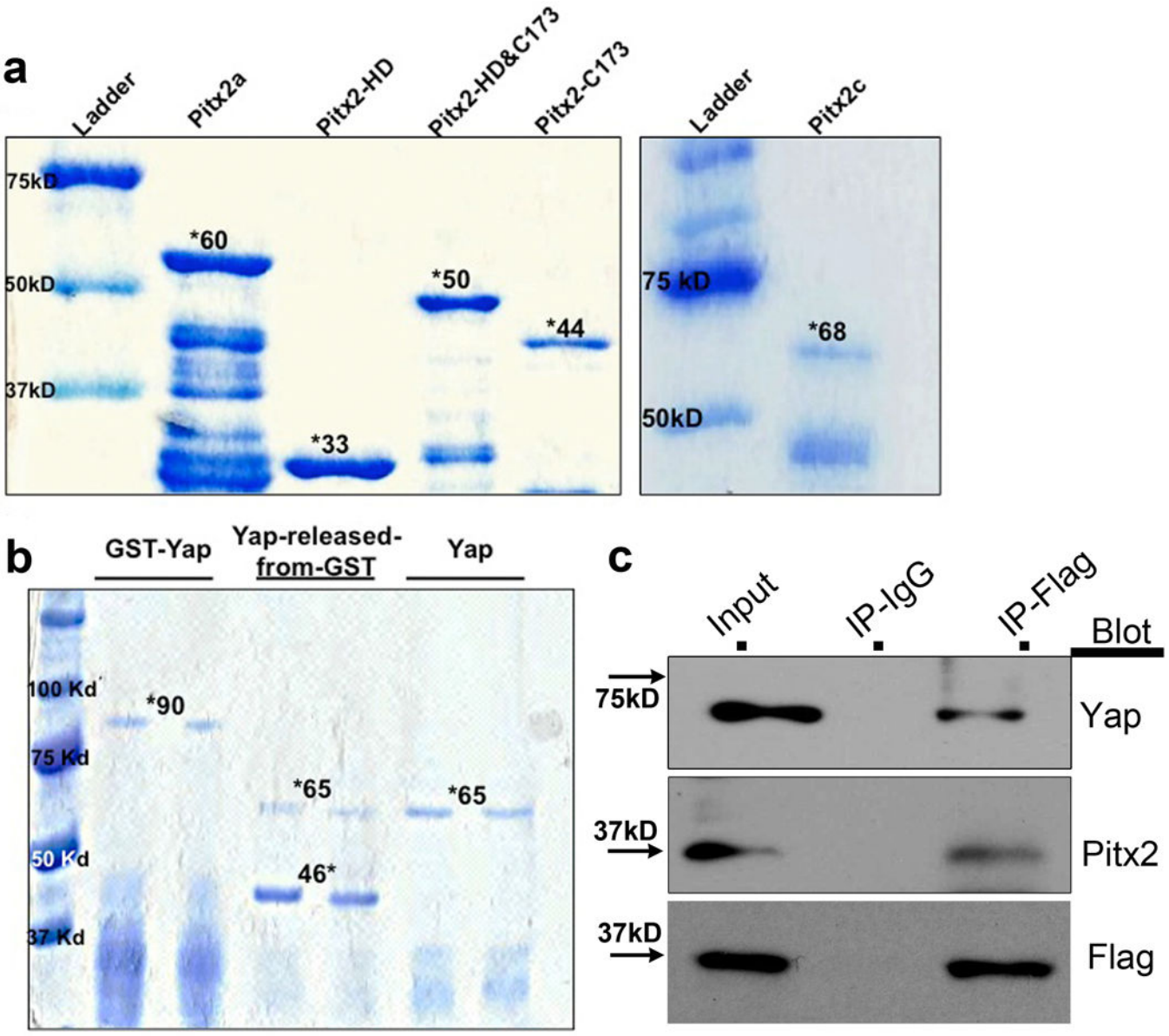

Extended Data Figure 5.

Generation of GST-tagged proteins and interaction between Pitx2 and Yap in vivo. (a) The mouse Pitx2a, Pitx2c, and truncated proteins were purified and run on 10% SDS-gel, coomassie blue staining showed the GST fusion protein band with correct size (marked by *). (b) Coomassie blue staining of the purified GST-Yap, Yap cut by prescission protease and pure Yap protein. (c) Co-IP of Flag in *Pitx2*^{flag} ventricles at 5 DPR, and blotting of Yap, Pitx2, and Flag.

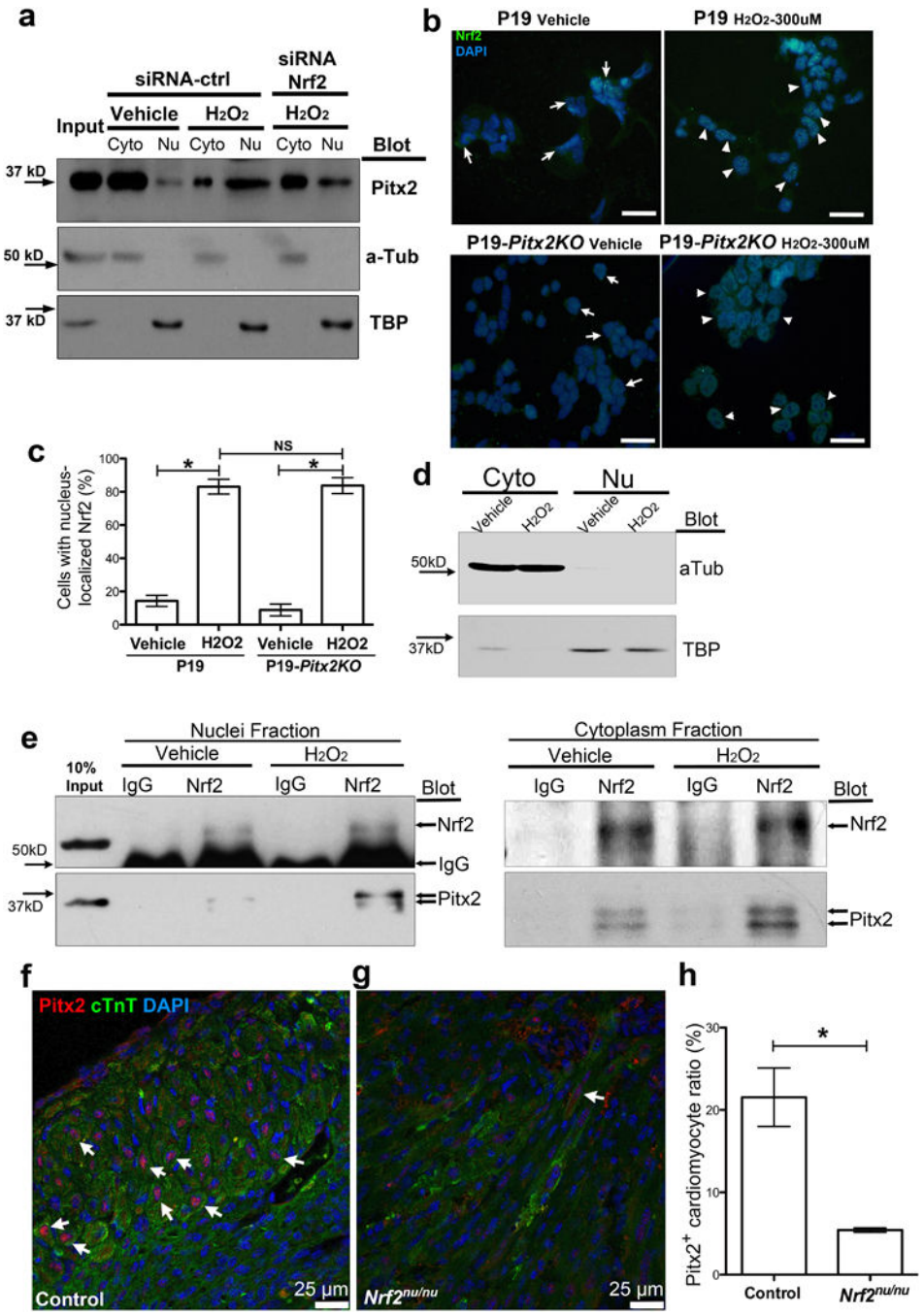

Extended Data Figure 6.

Nuclei-shuttling of Nrf2 is independent of *Pitx2*. (a) Blotting of Pitx2, α-Tubulin, and TATA-binding protein (TBP) of P19 cell fraction after H_2O_2, with or without *Nrf2* siRNA treatment. (b) Immunofluorescent staining of Nrf2 (green) in P19 and P19-*Pitx2KO* cells after vehicle or H_2O_2 treatment. DAPI, blue. Scale bar, 50 μm. (c) The ratio of cells with nuclear Nrf2 over total cell number, n=6. (d) Blotting of α-Tubulin and TBP to show cell fraction of P19 cells used in (e). (e) Co-IP Nrf2 from nuclear and cytoplasmic fraction of P19 cells after vehicle or H_2O_2 treatment, blotting shows Nrf2 and Pitx2. (f–h) 4 DPMI

control (*C57BL6*) (f) and *Nrf2*$^{nu/nu}$ (g) cross-sections stained for Pitx2 (red), cTnT (green), and DAPI (blue), with the ratio of cardiomyocytes with nuclei-localized Pitx2 quantified in h, n=4. Arrows, Pitx2^{+} cardiomyocyte. Mean ± S.E.M.; Statistical test, (c) one-way ANOVA plus Bonferroni post-test; (h) Mann-Whitney. *, p<0.05; NS, not significant.

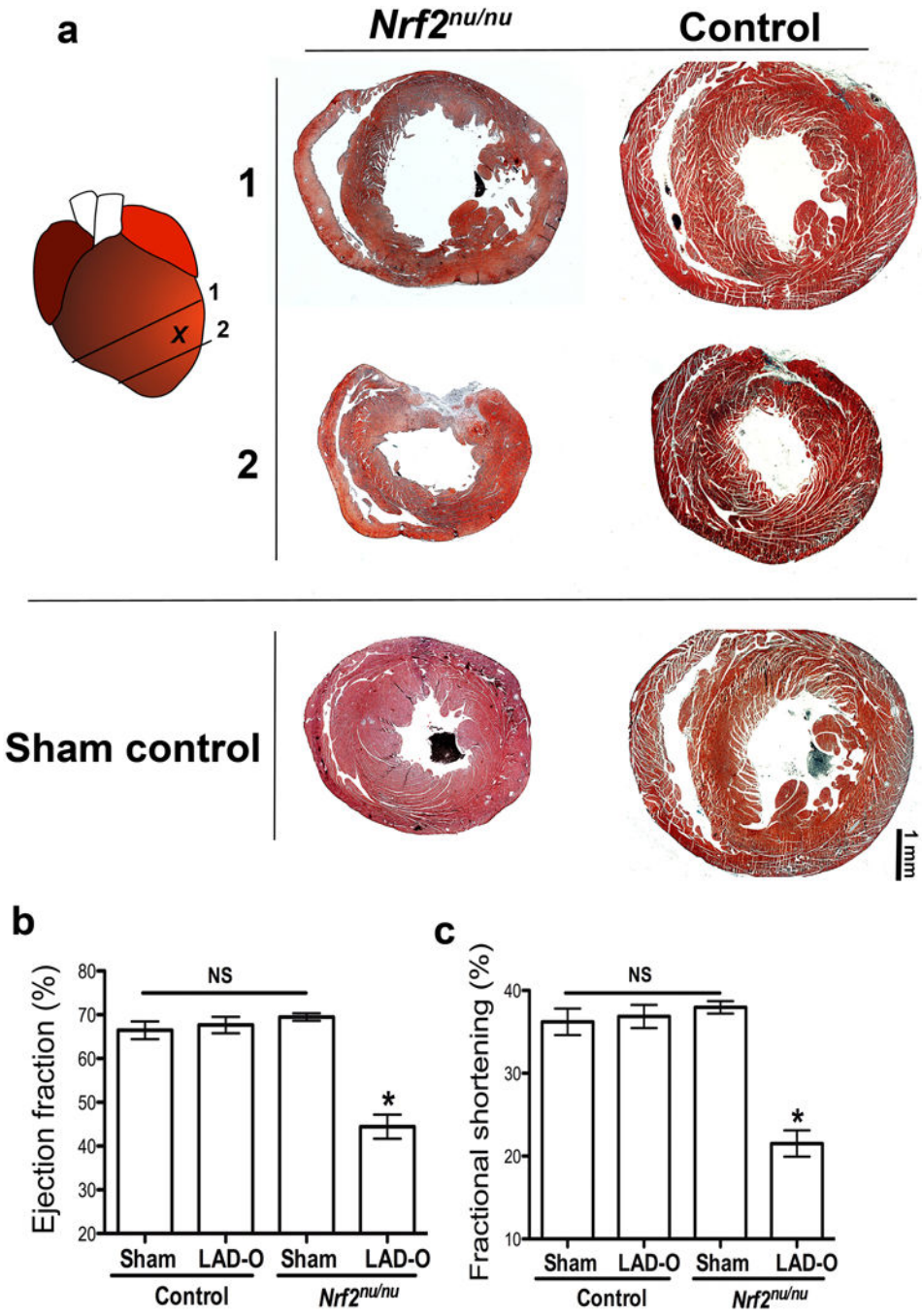

Extended Data Figure 7.

Nrf2 is required for neonatal myocardial regeneration. (a) Trichrome images of *Nrf2*$^{nu/nu}$ and control heart (*C57BL6*) at 21 days after P2 LAD-O, along with sham controls. (b, c)

Ejection fraction (b) and fractional shortening (c) of LAD-O and sham hearts. Mean ± S.E.M.; Statistical test, (b, c) Mann-Whitney. *, p<0.05; NS, not significant.

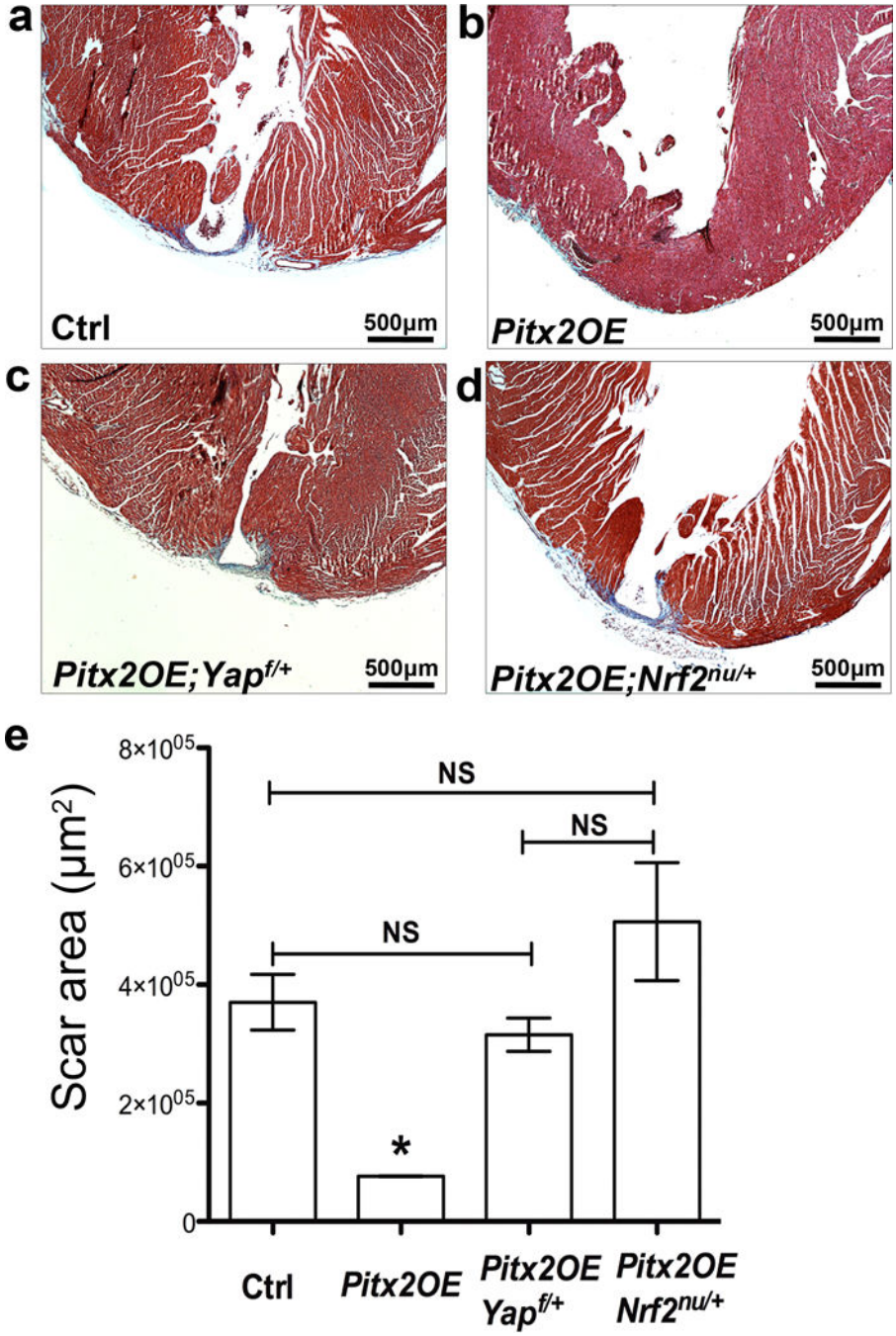

Extended Data Figure 8.

Yap and *Nrf2* are essential for *Pitx2*-induced myocardial regeneration. (a–d) Trichrome staining showing apical scarring of different groups at 28 DPR, apex resection was performed at P8. (e) Quantification of scar area, n=4. Mean ± S.E.M.; Statistical test, (e) Mann-Whitney. *, p<0.05 compared to other three groups; NS, not significant.

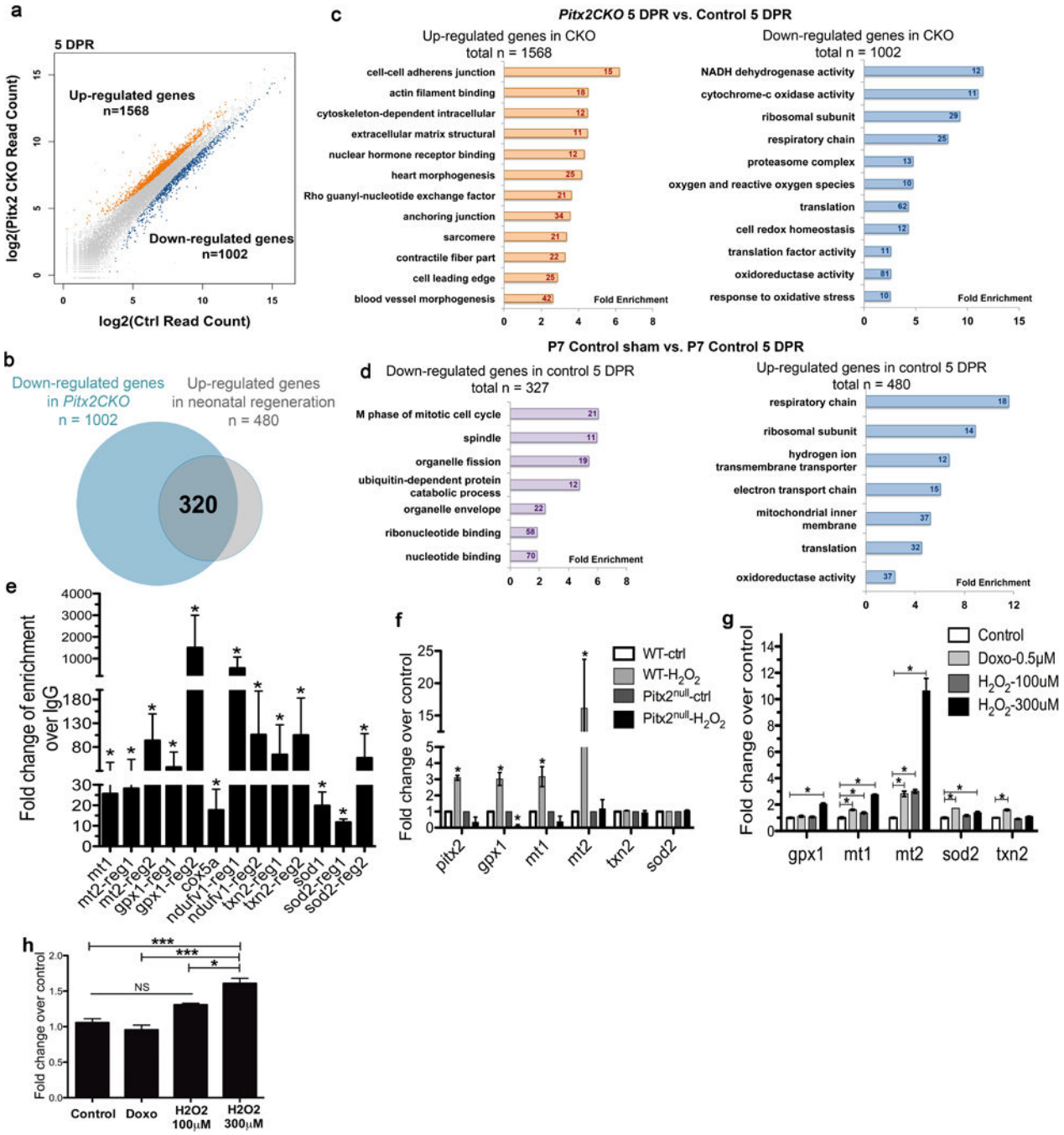

Extended Data Figure 9.

Pitx2 regulates antioxidant scavenger genes. (a) Overall change of genes in *Pitx2CKO* compared to control. (b) Up-regulated genes in 5 DPR control over wild type sham heart (n=480) overlaid with down-regulated genes in 5 DPR *Pitx2CKO* over 5 DPR control heart (n=1002). (c) GO-analysis of genes up-regulated (left) and down-regulated (right) in *Pitx2CKO* ventricles over controls at 5 DPR. (d) GO-analysis of genes up-regulated (right) and down-regulated (left) in 5 DPR control ventricles over age matching sham hearts. (e) ChIP-qPCR confirming the binding of Pitx2 to the regulatory regions of target genes, n=4.

(f) qPCR detecting *Pitx2* and antioxidant genes in wild type and *pitx2*$^{nu/nu}$ embryonic stem cells after vehicle or H_2O_2 treatment, n=4. (g) qPCR of antioxidant genes in P19 cells after doxorubicin or H_2O_2 treatment, n=5. (h) qPCR of *Pitx2* in P19 cells after doxorubicin or H_2O_2 treatment, n=5. Mean ± S.E.M.; Statistical test, (e–h) Mann-Whitney. *, p<0.05; ***, p<0.001; NS, not significant.

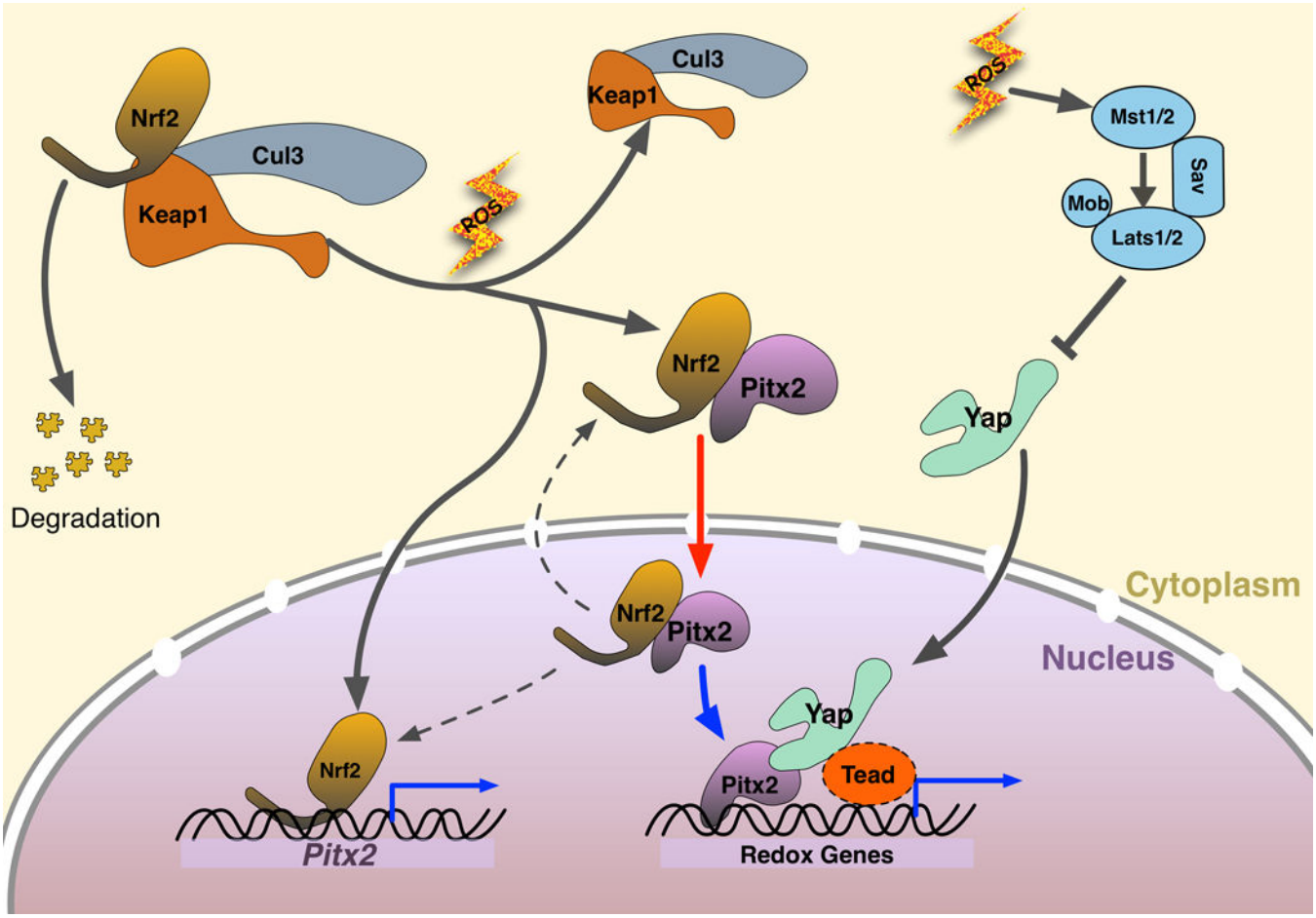

Extended Data Figure 10.

Mechanism model of *Pitx2*, *Nrf2*, and *Yap* responding to oxidative stress. When oxidative stress is low, Nrf2 is sequestered in cytoplasm by its degradation complex (Cul3, Keap1), and Pitx2 stays either in cytoplasm or at low expression level. When redox balance is disturbed by ROS, Nrf2 breaks away from degradation complex, and enter nuclei to up-regulate *Pitx2*, Nrf2 also binds cytoplasmic Pitx2 and shuttle it to nuclei, where Pitx2 and Yap co-regulate their common targets including critical antioxidant genes. In wild type adult mouse heart, active Yap is maintained at a low level, even after ischemic injury, thus not able to repair myocardium efficiently. When *Pitx2* is over-expressed in cardiomyocytes, sufficient amount of Pitx2 will cooperate with low level of resident active Yap to induce the expression of beneficial antioxidant scavengers in a synergetic pattern, rendering protection to injured myocardium. Red arrow, supported by *in vitro* evidence; Blue arrows, supported by *in vivo* evidence.

Supplementary Material

Refer to Web version on PubMed Central for supplementary material.

Acknowledgments

The project was supported in part by IDDRC grant number 1U54 HD083092 from the Eunice Kennedy Shriver National Institute of Child Health & Human Development. This project was supported by the Mouse Phenotyping Core at Baylor College of Medicine with funding from the NIH (U54 HG006348). The project was also supported by grants from the National Institutes of Health (NIH)[DE 023177 and HL 118761 to J.F.M., DE 13941 to B.A.A], the Vivian L. Smith Foundation [J.F.M.]. J.F.M. was supported by Transatlantic Network of Excellence Award LeDucq Foundation Transatlantic Networks of Excellence in Cardiovascular Research 14CVD01: “Defining the genomic topology of atrial fibrillation”. G.T. was supported by AHA 13POST17040027 [G.T.]. P.C.K was supported by German Research Foundation (DFG) (KA4018/1-1).

References

1. Xin M, Olson EN, Bassel-Duby R. Mending broken hearts: cardiac development as a basis for adult heart regeneration and repair. Nat Rev Mol Cell Biol. 2013; 14:529–541. DOI: 10.1038/nrm3619 [PubMed: 23839576]
2. Porrello ER, et al. Transient regenerative potential of the neonatal mouse heart. Science. 2011; 331:1078–1080. doi:331/6020/1078 [pii] 10.1126/science.1200708. [PubMed: 21350179]
3. Itoh K, et al. Keap1 represses nuclear activation of antioxidant responsive elements by Nrf2 through binding to the amino-terminal Neh2 domain. Genes Dev. 1999; 13:76–86. [PubMed: 9887101]
4. Heallen T, et al. Hippo signaling impedes adult heart regeneration. Development. 2013; 140:4683–4690. [PubMed: 24255096]
5. Semina EV, et al. Cloning and characterization of a novel bicoid-related homeobox transcription factor gene, RIEG, involved in Rieger syndrome. Nat Genet. 1996; 14:392–399. [PubMed: 8944018]
6. Lu MF, Pressman C, Dyer R, Johnson RL, Martin JF. Function of Rieger syndrome gene in left-right asymmetry and craniofacial development. Nature. 1999; 401:276–278. DOI: 10.1038/45797 [PubMed: 10499585]
7. Wang J, et al. Pitx2 prevents susceptibility to atrial arrhythmias by inhibiting left-sided pacemaker specification. Proc Natl Acad Sci U S A. 2010; 107:9753–9758. doi:0912585107 [pii] 10.1073/pnas.0912585107. [PubMed: 20457925]
8. Kirchhof P, et al. PITX2c is expressed in the adult left atrium, and reducing Pitx2c expression promotes atrial fibrillation inducibility and complex changes in gene expression. Circulation Cardiovascular genetics. 2011; 4:123–133. DOI: 10.1161/CIRCGENETICS.110.958058 [PubMed: 21282332]
9. Giudice J, et al. Alternative splicing regulates vesicular trafficking genes in cardiomyocytes during postnatal heart development. Nature communications. 2014; 5:3603.
10. Nord AS, et al. Rapid and pervasive changes in genome-wide enhancer usage during mammalian development. Cell. 2013; 155:1521–1531. DOI: 10.1016/j.cell.2013.11.033 [PubMed: 24360275]
11. Bruning JC, et al. A muscle-specific insulin receptor knockout exhibits features of the metabolic syndrome of NIDDM without altering glucose tolerance. Mol Cell. 1998; 2:559–569. doi:S1097-2765(00)80155-0 [pii]. [PubMed: 9844629]
12. Chan K, Lu R, Chang JC, Kan YW. NRF2, a member of the NFE2 family of transcription factors, is not essential for murine erythropoiesis, growth, and development. Proc Natl Acad Sci U S A. 1996; 93:13943–13948. [PubMed: 8943040]
13. Xin M, et al. Hippo pathway effector Yap promotes cardiac regeneration. Proc Natl Acad Sci U S A. 2013; 110:13839–13844. doi:1313192110 [pii] 10.1073/pnas.1313192110. [PubMed: 23918388]
14. L’Honore A, et al. Redox regulation by Pitx2 and Pitx3 is critical for fetal myogenesis. Dev Cell. 2014; 29:392–405. DOI: 10.1016/j.devcel.2014.04.006 [PubMed: 24871946]

15. Dhalla NS, Temsah RM, Netticadan T. Role of oxidative stress in cardiovascular diseases. J Hypertens. 2000; 18:655–673. [PubMed: 10872549]
16. Larsson NG, Clayton DA. Molecular genetic aspects of human mitochondrial disorders. Annual review of genetics. 1995; 29:151–178. DOI: 10.1146/annurev.ge.29.120195.001055
17. Yue F, et al. A comparative encyclopedia of DNA elements in the mouse genome. Nature. 2014; 515:355–364. DOI: 10.1038/nature13992 [PubMed: 25409824]
18. Zanconato F, et al. Genome-wide association between YAP/TAZ/TEAD and AP-1 at enhancers drives oncogenic growth. Nat Cell Biol. 2015; 17:1218–1227. DOI: 10.1038/ncb3216 [PubMed: 26258633]
19. Galli GG, et al. YAP Drives Growth by Controlling Transcriptional Pause Release from Dynamic Enhancers. Mol Cell. 2015; 60:328–337. DOI: 10.1016/j.molcel.2015.09.001 [PubMed: 26439301]
20. Stein C, et al. YAP1 Exerts Its Transcriptional Control via TEAD-Mediated Activation of Enhancers. PLoS Genet. 2015; 11:e1005465. [PubMed: 26295846]
21. Morikawa Y, et al. Actin cytoskeletal remodeling with protrusion formation is essential for heart regeneration in Hippo-deficient mice. Sci Signal. 2015; 8:ra41. [PubMed: 25943351]
22. Puente BN, et al. The oxygen-rich postnatal environment induces cardiomyocyte cell-cycle arrest through DNA damage response. Cell. 2014; 157:565–579. DOI: 10.1016/j.cell.2014.03.032 [PubMed: 24766806]
23. Chouchani ET, et al. Ischaemic accumulation of succinate controls reperfusion injury through mitochondrial ROS. Nature. 2014; 515:431–435. DOI: 10.1038/nature13909 [PubMed: 25383517]
24. Shao D, et al. A functional interaction between Hippo-YAP signalling and FoxO1 mediates the oxidative stress response. Nature communications. 2014; 5:3315.

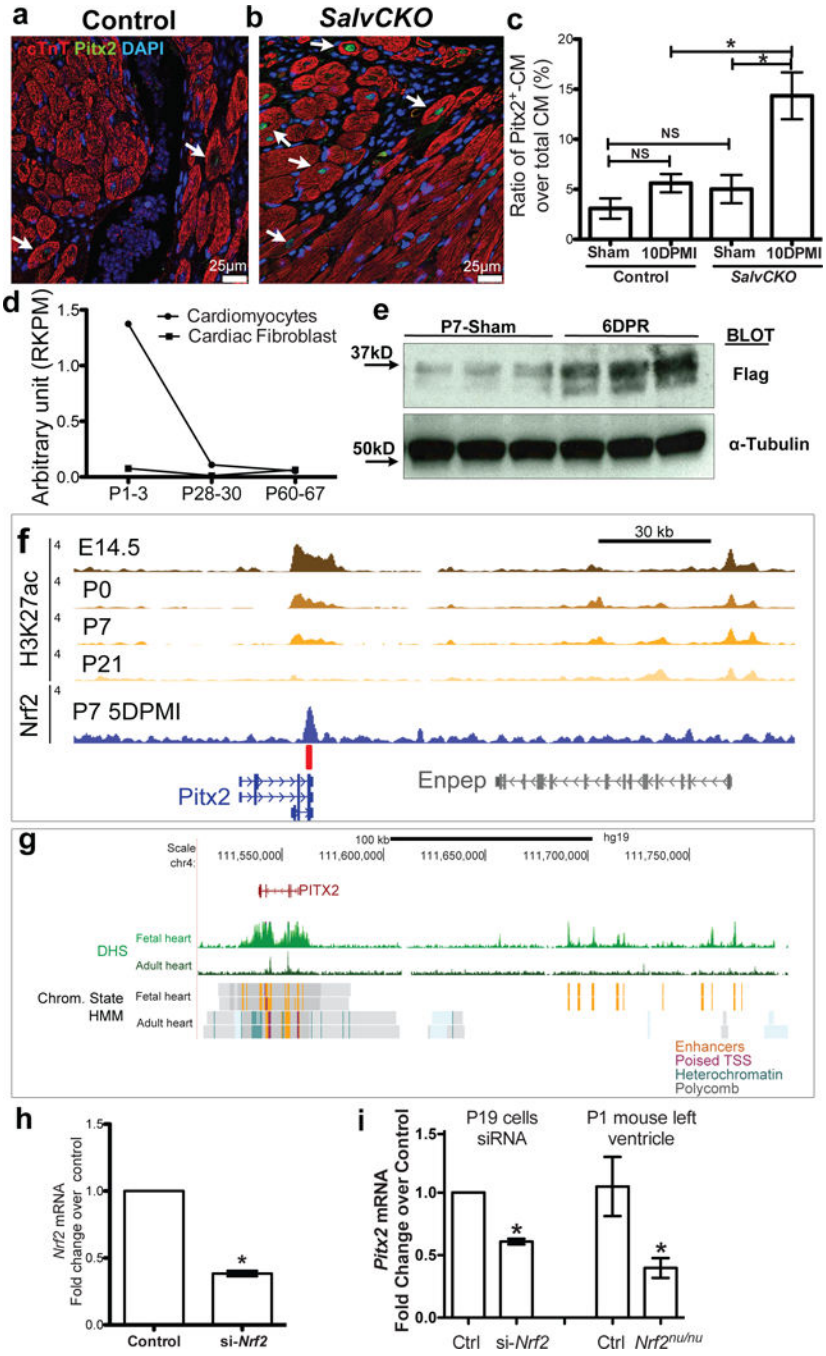

Figure 1.

Pitx2 is induced in injured myocardial. (a–c) Border zone of *SalvCKO* (b) and control (a) hearts stained for Pitx2 (green), cTnT (red), and DAPI (blue) at 10 day-post-MI, with Pitx2^{+} cardiomyocyte ratio quantified in c, n=4. (d) *Pitx2* expression showed by RNA-Seq, P, postnatal day. (e) Western blot of Flag and a-Tubulin in 5 DPR *Pitx2*^{flag} ventricles, resected at P1. (f) Nrf2 directly binds to *Pitx2* enhancer after LAD-O. The heart specific enhancers are marked by H3K27ac ChIP-Seq. red bar, Nrf2 binding element. (g) DHS-Seq and chromatin state tracks of fetal and adult human heart tissue. Orange color indicates active

enhancer regions. (h) qPCR showed knocking-down of *Nrf2* by siRNA in P19 cells, n=4. (i) qPCR of *Pitx2* in P19 cells with siRNA targeting *Nrf2*, and $Nrf2^{nu/nu}$ heart, compared to controls, n=4. Mean ± S.E.M.; Statistical test, (c) one-way ANOVA plus Bonferroni post-test; (i, right part) Mann-Whitney; (h, i left part) see Methods; *, $p<0.05$; NS, not significant.

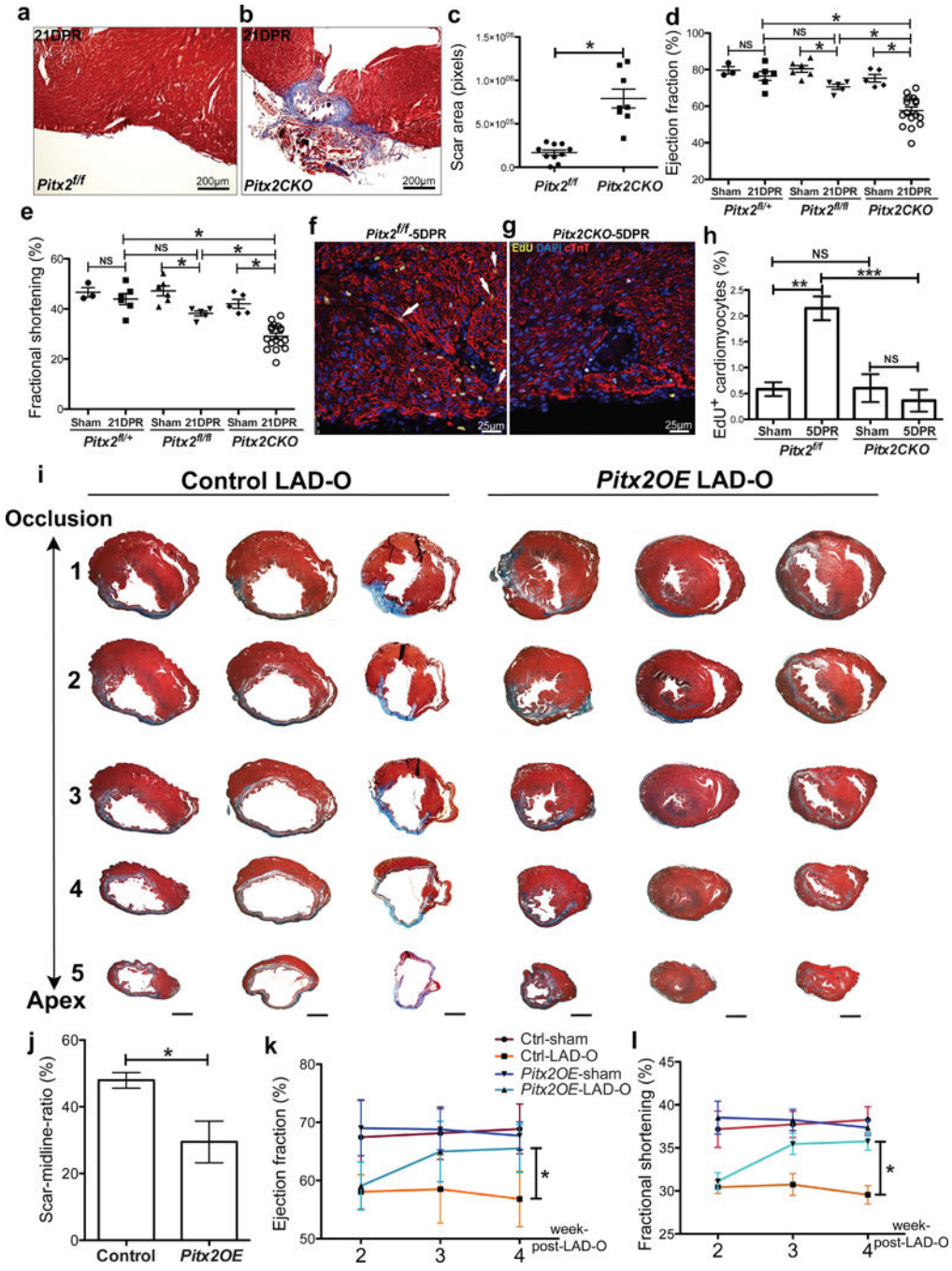

Figure 2.

Pitx2 is required and sufficient to promote myocardial regeneration. (a–c) Trichrome-stained *Pitx2*$^{f/f}$ (a) and *Pitx2CKO* (b) apex at 21 DPR, with scar size quantified in c. (d, e) Echocardiography showed the ejection fraction (d) and fractional shorting (e) at 21 DPR. (f–h) 5 DPR *Pitx2*$^{f/f}$ (f) and *Pitx2CKO* (g) apical sections stained for EdU (yellow), cTnT (red), and DAPI (blue). Arrow, EdU^{+} cardiomyocyte. Cardiomyocyte proliferative ratio was quantified in h, n=4. (i) Serial transverse heart sections at 5 weeks post-LAD-O, performed at 8weeks. (j) Percentage of fibrotic left ventricular myocardium quantified at 5 weeks post-

LAD-O, n=5. Scale bar, 1mm. (k, l) Ejection fraction (k) and fractional shortening (l) of LAD-O and sham hearts. Mean ± S.E.M.; Statistical test, (d, e) one-way ANOVA plus Bonferroni post-test; (c, h, j–l) Mann-Whitney; *, $p<0.05$; NS, not significant.

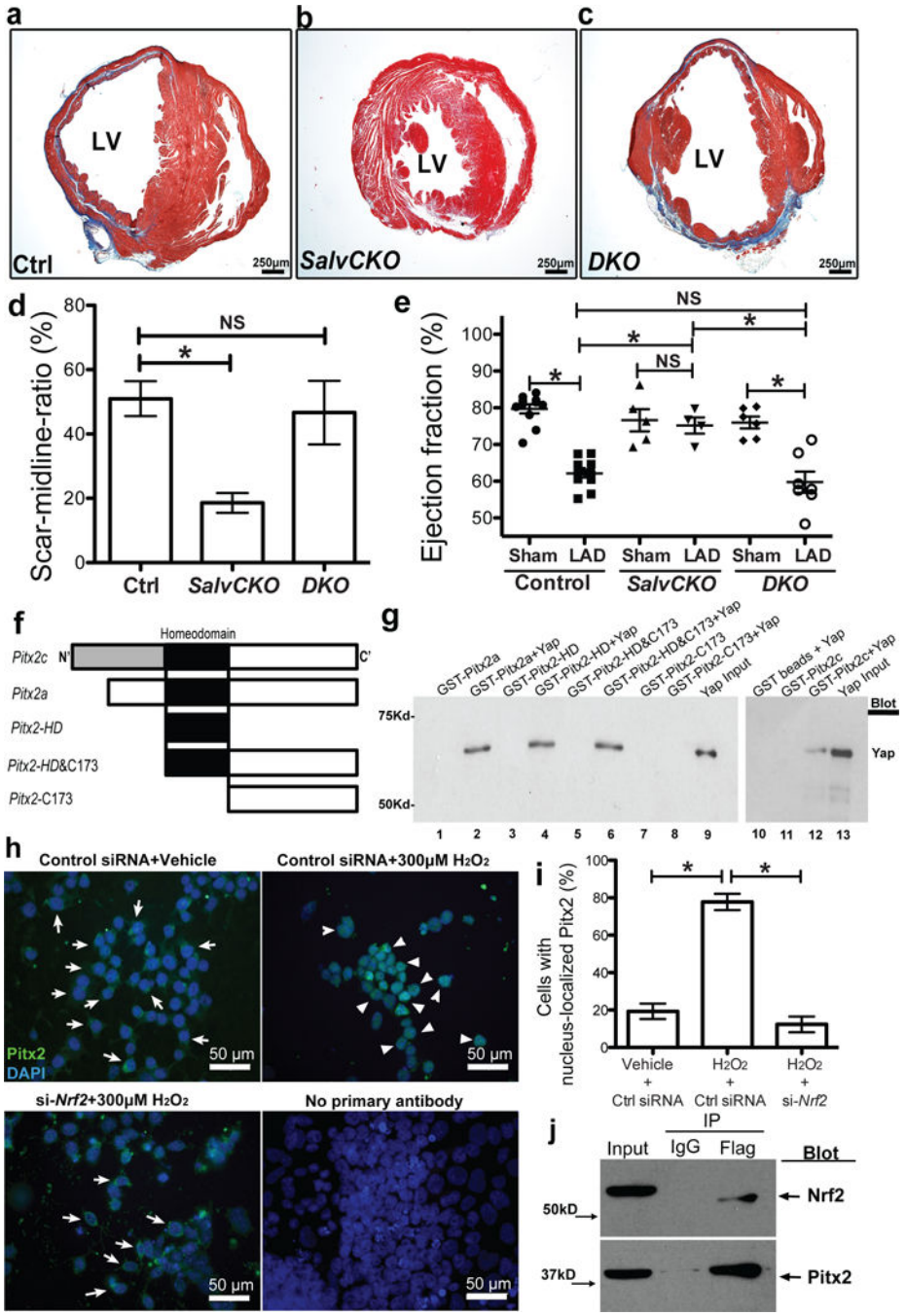

Figure 3.

Pitx2 interacts with Yap in regenerating hearts, and its nuclear shuttling requires Nrf2. (a–d) Trichrome-stained control (*Salv*$^{f/f}$;*Pitx2*$^{f/f}$) (a), *SalvCKO* (b) and *DKO* (c) sections at 28 days after P8 LAD-O with scar size quantification (d), n=4. (e) Echocardiography showed ejection fraction. (f) Diagram of *GST-Pitx2* constructs. (g) *GST-Pitx2* pull-down assay. Yap was detected by Western blotting. (h–i) Immunofluorescent staining of Pitx2 (green) and DAPI (blue) in P19 cells after vehicle or H_2O_2 treatment, with control siRNA or siRNA targeting *Nrf2*. Arrow, cytoplasmic staining; arrowhead, nuclear staining. The ratio of cells

with nucleus-localized Pitx2 over total cell number is quantified in i. (j) Co-IP of Flag in 5 DPR *Pitx2*^{flag} ventricles, resected at P1, blotting of Nrf2 and Pitx2. Mean ± S.E.M.; Statistical test, (e) one-way ANOVA plus Bonferroni post-test; (d, i) Mann-Whitney; *, $p<0.05$; NS, not significant.

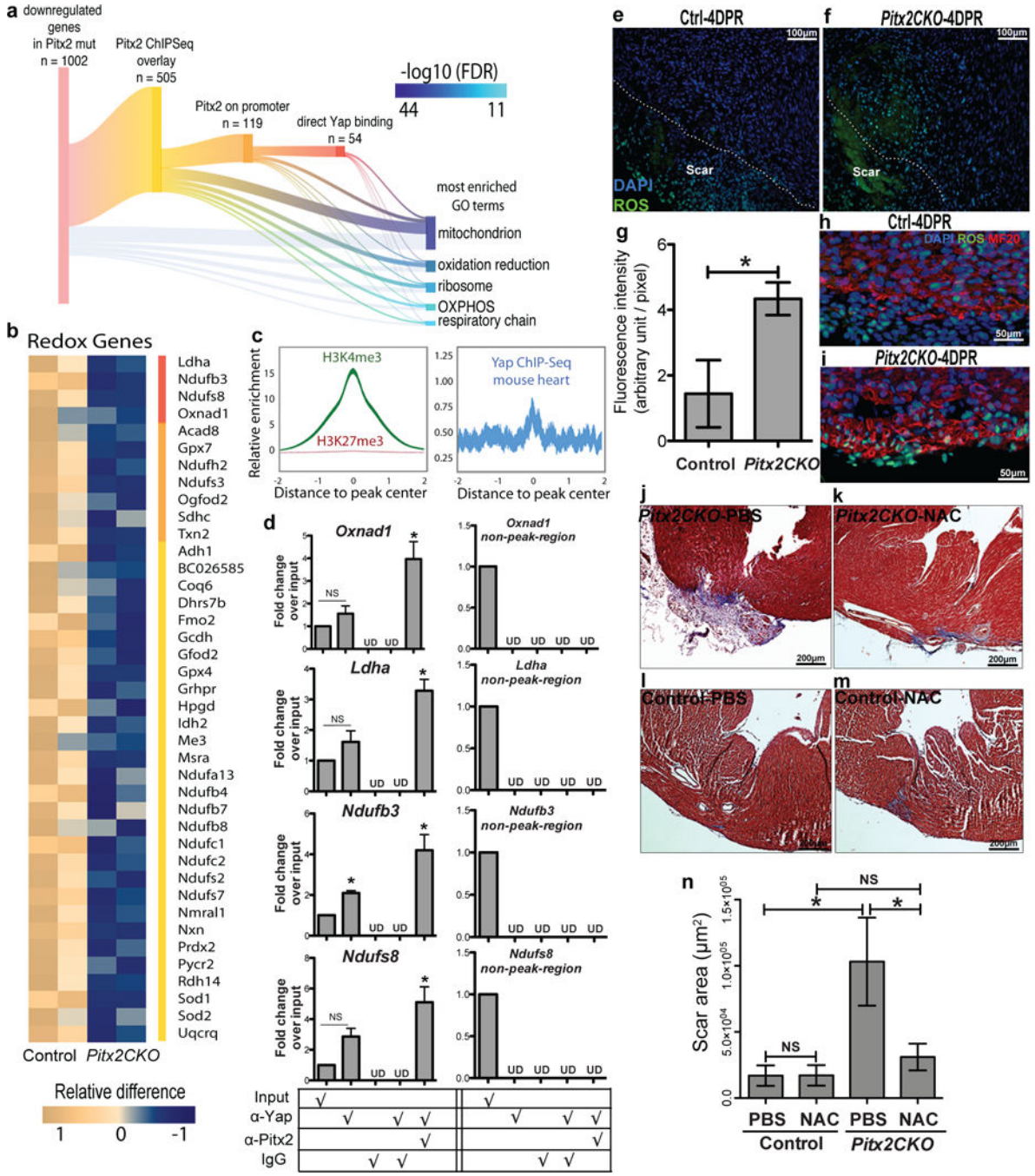

Figure 4.

Pitx2 regulates redox balance in neonatal myocardium. (a) Sankey diagram shows direct target genes of *Pitx2* from overlaying ChIP-Seq and RNA-Seq profiles. A subset of genes is further branched according to promoter binding activity of Pitx2 and Yap. Gene ontology analysis is performed on 1002 down-regulated genes in *Pitx2CKO* ventricles at 5 days after P1 resection. The GO terms are listed by significance in descending order. The branches indicate the source of genes for each term. OXPHOS, oxidative phosphorylation. (b) Heat map highlights mitochondrial genes directly targeted by Pitx2. Red bar, genes co-regulated

by Pitx2 and Yap; orange, direct binding of Pitx2 on promoters. (c) Heart specific H3K4me3 ChIP-Seq and Yap ChIP-Seq read distribution with in 2 kb interval of promoter region of *Pitx2* direct target genes. The width of the curve indicate 95% confidence interval. (d) ChIP-re-ChIP showing co-occupancy of Pitx2 and Yap at the regulatory regions of common target genes (in b, red bar), n=3. (e–i) ROS staining (green) of apical border zone in *Pitx2CKO* (f, i) and control (e, h), with fluorescent intensity quantified in g. MF20, red; DAPI, blue, n=4. (j–n) Trichrome at 21DPR showed apical scarring of *Pitx2CKO* (j, k) and control (l, m) hearts treated with PBS (j, l) or NAC (k, m), with scar area quantified in n, n=5. Mean ± S.E.M.; Statistical test, (n) one-way ANOVA plus Bonferroni post-test; (g) Mann-Whitney; (d) Mann-Whitney and Wilcoxon signed-rank test; *, $p<0.05$; NS, not significant.